A climate model of intermediate complexity: Physical consistence and applications

Erich Becker

Urs Schaefer-Rolffs, Sebastian Brune, Mark Schlutow, Rahel Knöpfel

Leibniz Institute of Atmospheric Physics at the University of Rostock (IAP)

Kühlungsborn, Germany

Why a mechanistic GCM, i.e., a GCM with intermediate complexity?

- Easily comprehensible, therefore allowing process studies by means of straightforward sensitivity experiments.
- Development and testing of parameterizations/closures and may be applied also in complex models (e.g., subgrid-scale diffusion)
- Good chance to achieve physical (or at least energetical) consistency.

…

When using comprehensive (complex) GCMs?

- Detailed climate studies with realistic parameters.
- Processes neglected in the mechanistic case matter.

…

Special focus of model development at IAP: **Representation of gravity waves (GWs) and macro-turbulent diffusion**

Reason:
GWs and turbulence are first-order dynamical processes in the mesosphere/lower thermosphere (MLT, 50-110 km)

Snapshot of temperature (K) and dissipation (K/d) around 85 km (January)

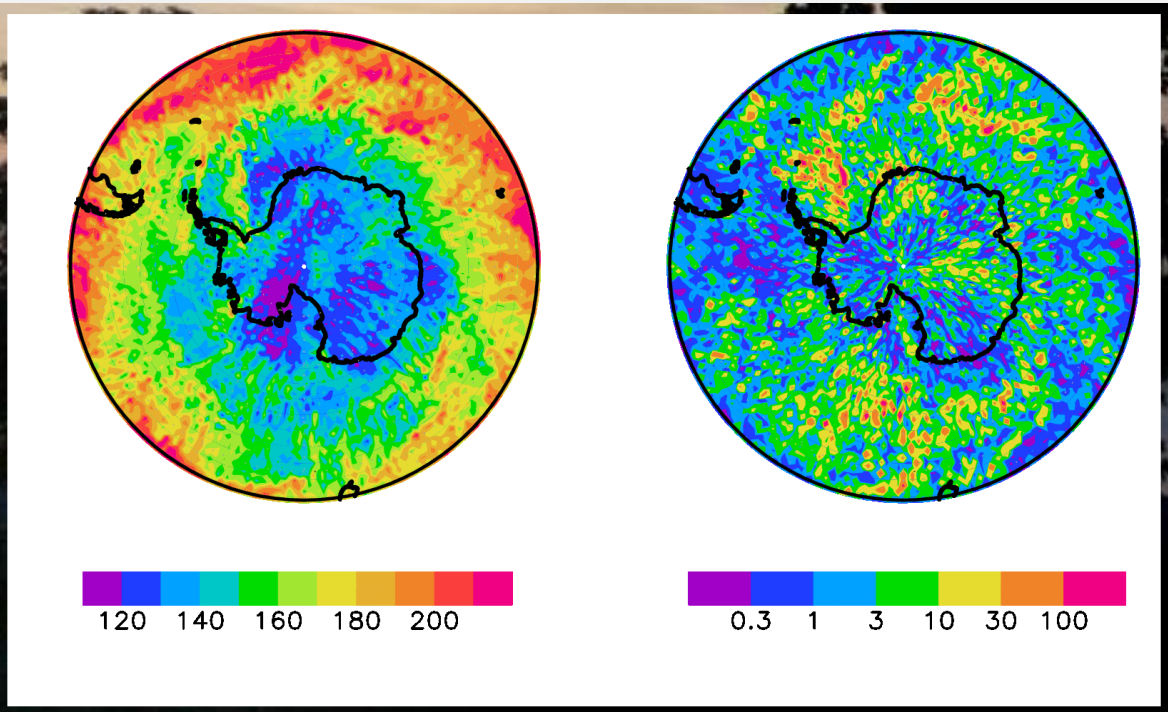

Lorenz energy cycle

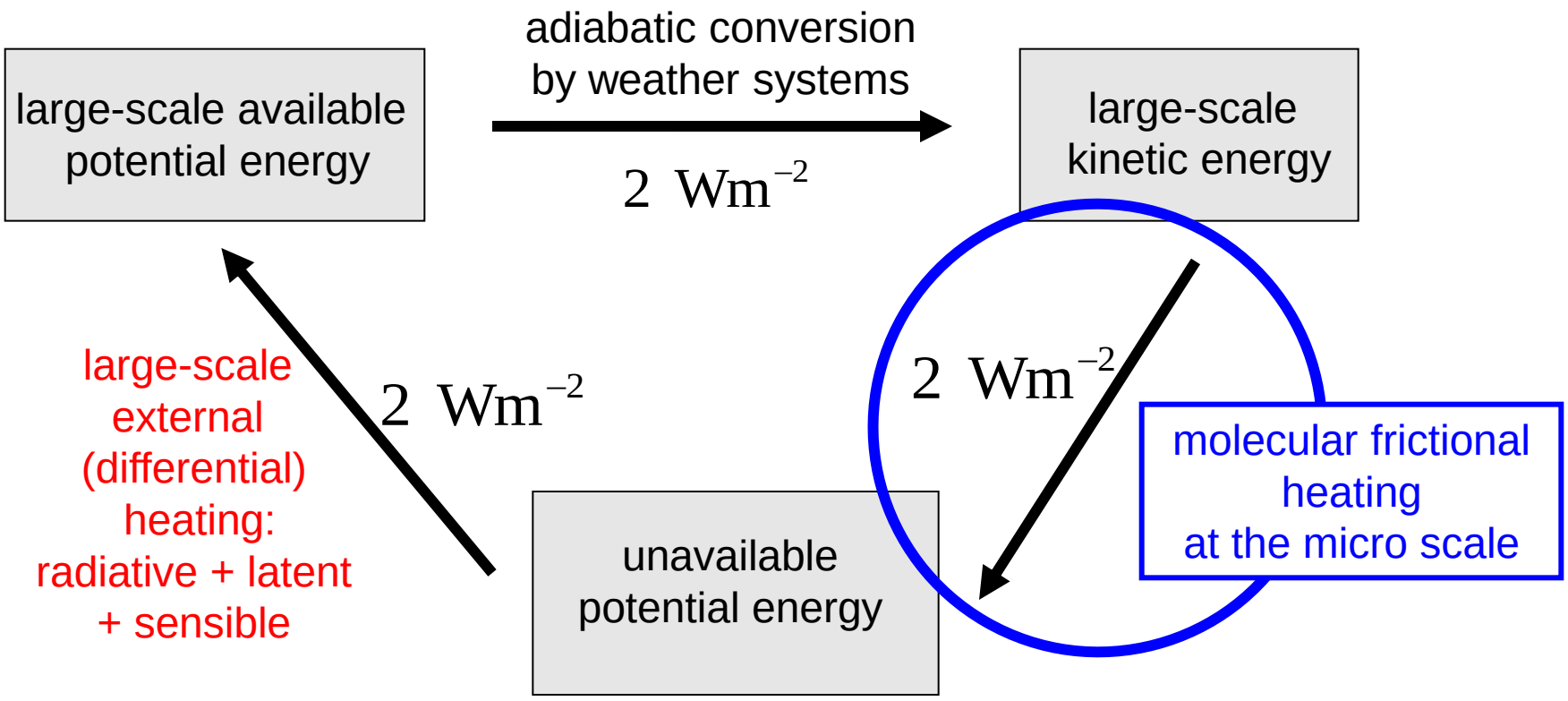

- frictional heating essential for entropy and energy budgets:
  net diabatic heating of the atmosphere = frictional heating (Lorenz, 1967)

- molecular frictional heating occurs at the end of energy cascades through the mesoscales (including GWs) and turbulence

Conventional GCM with a diagnostic turbulence model

$$d_t \mathbf{v} = -f\,\mathbf{e}_z \times \mathbf{v} - \frac{\nabla p}{\rho} + \rho^{-1}\,\partial_z\,(\rho\,K_z\,\partial_z \mathbf{v}\,) + \{\text{hyperdiffusion}\}$$

$$d_t h = \frac{d_t p}{\rho} + Q_{rad} + Q_{lat} + \frac{c_p}{\rho}\,\partial_z\,(\rho\,\frac{T}{\Theta} K_z\,\partial_z \Theta\,) - \mathbf{v}\cdot\frac{\partial_z\,(\rho\,K_z\;\partial_z \mathbf{v}\,)}{\rho}\,, \quad h = c_p\,T$$

- K_z and dynamic boundary conditions as usual
- $\{\text{hyperdiffusion}\}$ without stress tensor; $-\mathbf{v}\cdot\frac{\partial_z\,(\rho\,K_z\,\partial_z \mathbf{v}\,)}{\rho}$ is flawed

Consistent formulation

$$d_t \mathbf{v} = -f\,\mathbf{e}_z \times \mathbf{v} - \frac{\nabla p}{\rho} + \rho^{-1}\,\partial_z\,(\rho\,K_z\,\partial_z \mathbf{v}) + \rho^{-1}\,\nabla\,(\rho\,K_h\,\mathsf{S}_h)$$

$$d_t h = \frac{d_t p}{\rho} + Q_{rad} + Q_{lat} + \frac{c_p}{\rho}\,\partial_z\,(\rho\,\frac{T}{\Theta} K_z\,\partial_z \Theta\,) + \underbrace{K_z\,(\partial_z \mathbf{v})^2}_{\geq\,0} + K_h\,(\,\mathsf{S}_h \nabla\,)\cdot\mathbf{v}$$

- $\mathsf{S}_h = \mathsf{S}_h^T$, $K_h\,(\,\mathsf{S}_h \nabla\,)\cdot\mathbf{v} \geq 0$, and $\mathsf{S}_h \mathbf{e}_z = 0$ (Becker, 2001, JAS)
- no exchange of mechanical energy between the surface and the the atmosphere $\rightarrow$ energy conserving discretization of vertical momentum diffusion and shear production (finite-difference analogue of the no-slip condition)

  (Burchard , 2002, OM; Becker, 2003, MWR; Boville & Bretherton, 2003, MWR)

Conventional GCM with a diagnostic turbulence model

$$d_t \mathbf{v} = -f\,\mathbf{e}_z \times \mathbf{v} - \frac{\nabla p}{\rho} + \rho^{-1}\,\partial_z\,(\rho\,K_z\,\partial_z \mathbf{v}\,) + \{\text{hyperdiffusion}\}$$

$$d_t h = \frac{d_t p}{\rho} + Q_{rad} + Q_{lat} + \frac{c_p}{\rho}\,\partial_z\,(\rho\,\frac{T}{\Theta} K_z\,\partial_z \Theta\,) - \mathbf{v}\cdot\frac{\partial_z\,(\rho\,K_z\;\partial_z \mathbf{v}\,)}{\rho}\,, \quad h = c_p\,T$$

- K_z and dynamic b
- {hyperdiffusion} w

Another issue: Heat diffusion based on potential temperature may violate the Second Law (Gassmann & Herzog, QJRMS, 2014)

Consistent formulation

$$d_t \mathbf{v} = -f\,\mathbf{e}_z \times \mathbf{v} - \frac{\nabla p}{\rho} + \rho^{-1}\,\partial_z\,(\rho\,K_z\,\partial_z \mathbf{v}) + \rho^{-1}\,\nabla\,(\rho\,K_h\,\mathsf{S}_h)$$

$$d_t h = \frac{d_t p}{\rho} + Q_{rad} + Q_{lat} + \frac{c_p}{\rho}\,\partial_z\,(\rho\,\frac{T}{\Theta} K_z\,\partial_z \Theta + \underbrace{K_z\,(\partial_z \mathbf{v})^2}_{\geq\,0} + K_h\,(\,\mathsf{S}_h \nabla\,)\cdot\mathbf{v}$$

- $\mathsf{S}_h = \mathsf{S}_h^T$, $K_h\,(\,\mathsf{S}_h \nabla\,)\cdot\mathbf{v} \geq 0$, and $\mathsf{S}_h \mathbf{e}_z = 0$ (Becker, 2001, JAS)
- no exchange of mechanical energy between the surface and the the atmosphere $\rightarrow$ energy conserving discretization of vertical momentum diffusion and shear production (finite-difference analogue of the no-slip condition)

  (Burchard , 2002, OM; Becker, 2003, MWR; Boville & Bretherton, 2003, MWR)

Kühlungsborn Mechanistic general Circulation Model (KMCM)

- standard spectral dynamical core; T120/L190 or T240/L190 up to 125 km; T330L100 up 60 km
- mechanistic because of simple representations of the diabatic heating rates due to radiation (temperature relaxation) and condensation

- hydrodynamically consistent parameterization of turbulent friction

$$\left(\partial_t \vec{v}\right)_{diff} = \frac{1}{\rho}\nabla\left(\rho\, K_h\, \vec{\vec{S}}\right) + \frac{1}{\rho}\,\partial_Z\left(\rho\,(K_Z+\upsilon)\,\partial_Z\,\vec{v}\right),\quad \vec{\vec{S}} = \vec{\vec{S}}^{\,T}\ \text{(ang. mom.)}$$

$$c_p\left(\partial_t T\right)_{diss} = K_h\,|\,\vec{\vec{S}}\,|^2 + (K_z+\upsilon)\,(\partial_Z \vec{v})^2 \geq 0 \qquad \text{(second law)}$$

- diffusion coefficients adjust automatically to dynamic instability

$$K_z = l_z^2\,|\,\partial_z v\,|\,F(Ri),\quad K_h = l_h^2\,|\,\vec{\vec{S}}\,|\,(1+\alpha\,F(Ri))$$

$$F(Ri) = \begin{cases} \sqrt{1-18Ri}, & Ri < 0 \\ (1+9Ri)^{-1}, & Ri \geq 0 \end{cases}$$

3 free parameters:
2 mixing lengths and α;

$$Ri = N^2/(\partial_z v)^2 \rightarrow Ri - 0.25 \ \text{ for } \ p < 100\ \text{hPa}$$

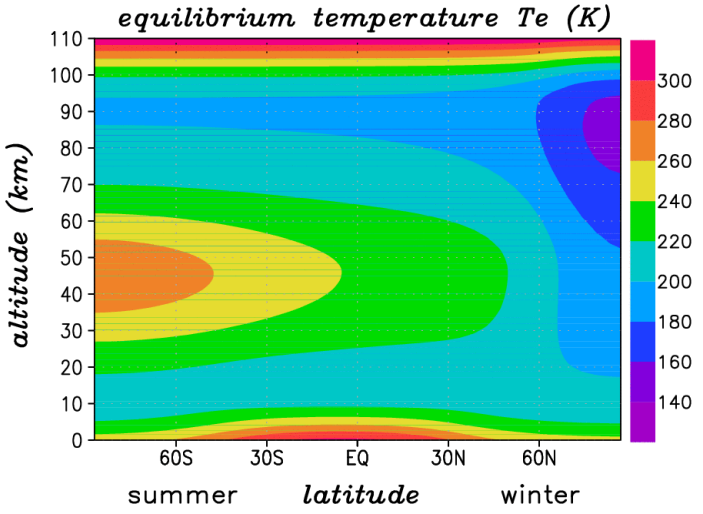

Assumed equilibirium state for January

Simulated dynamically determined January climatology

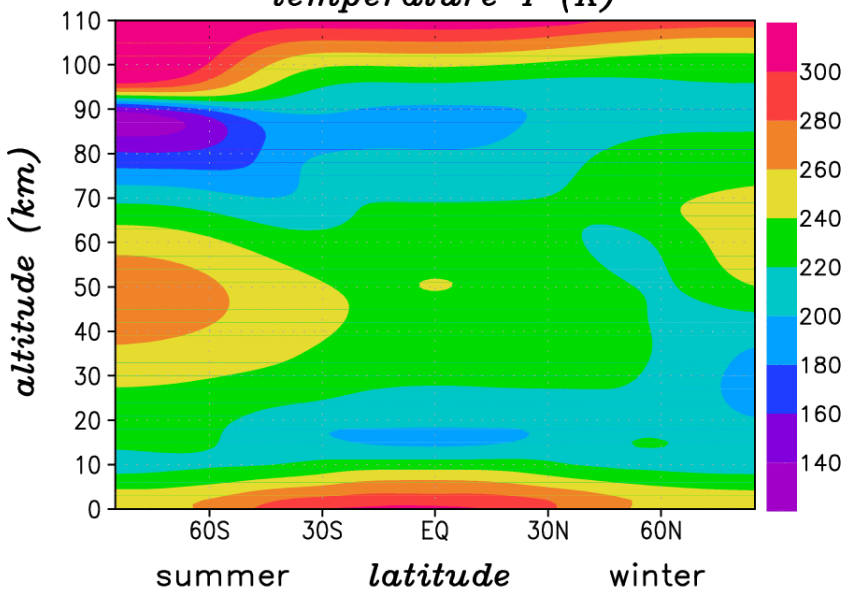

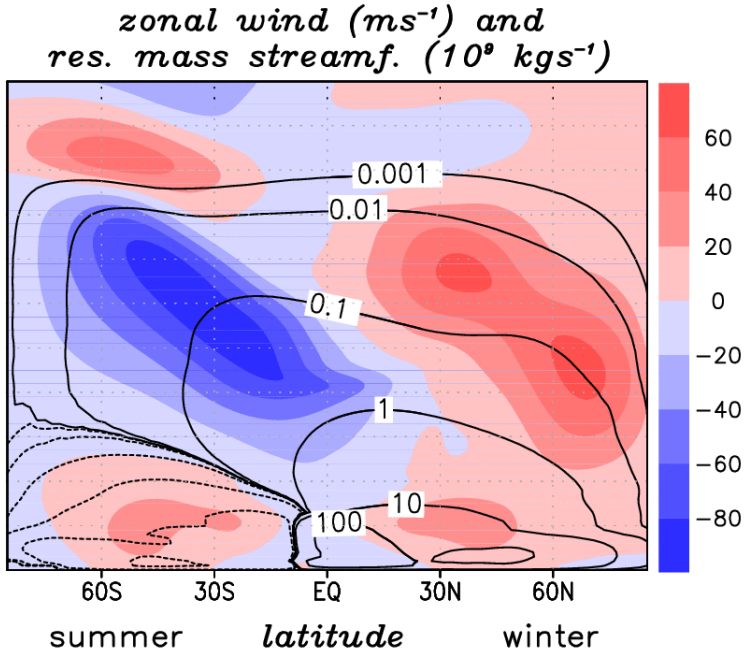

Gravity waves and planetary waves around the summer mesopause: Temperature at 0.003 hPa (~85 km) for different filtering of horizontal scales

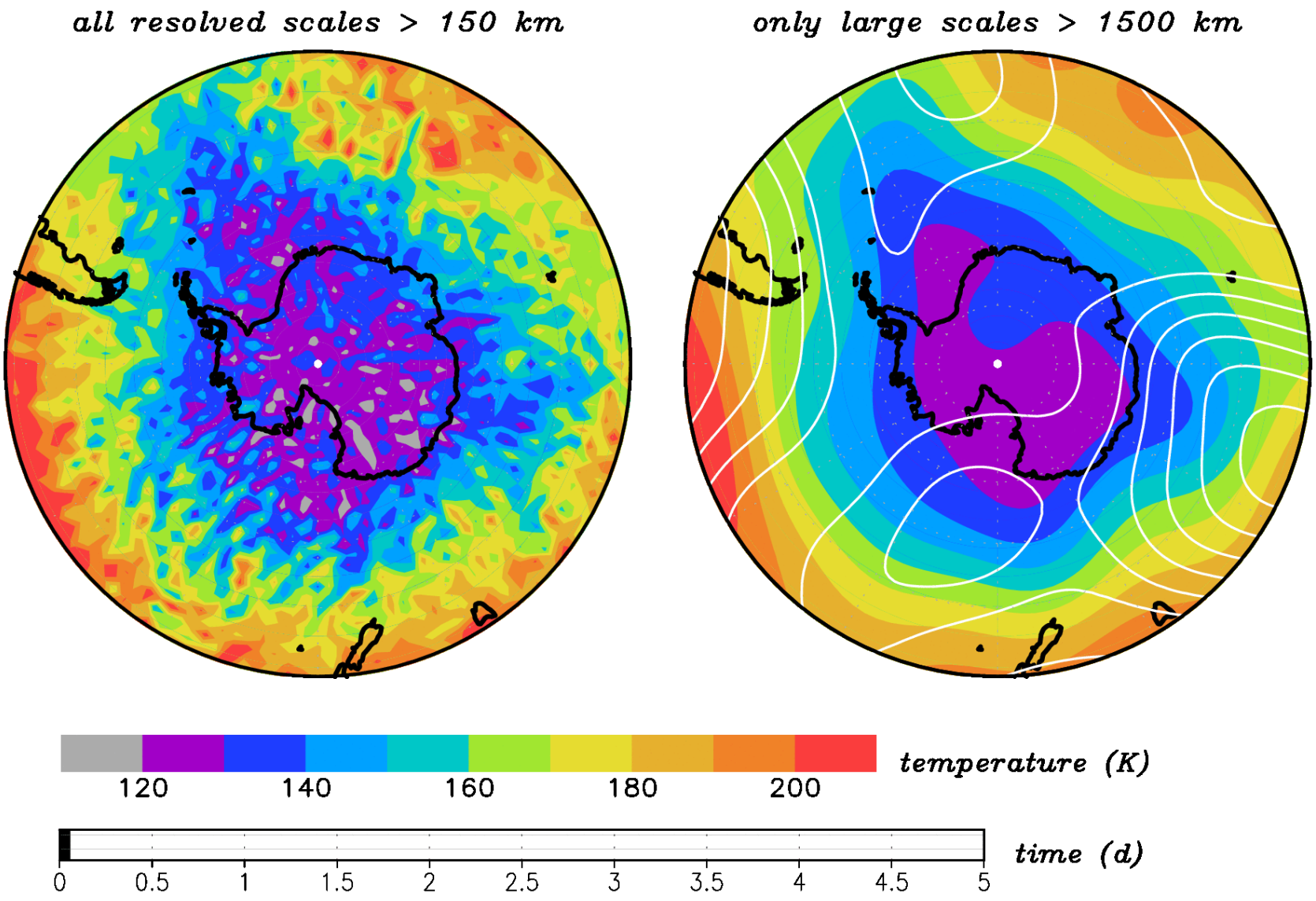

Snapshots of the simulated vertical wind in the summer hemisphere

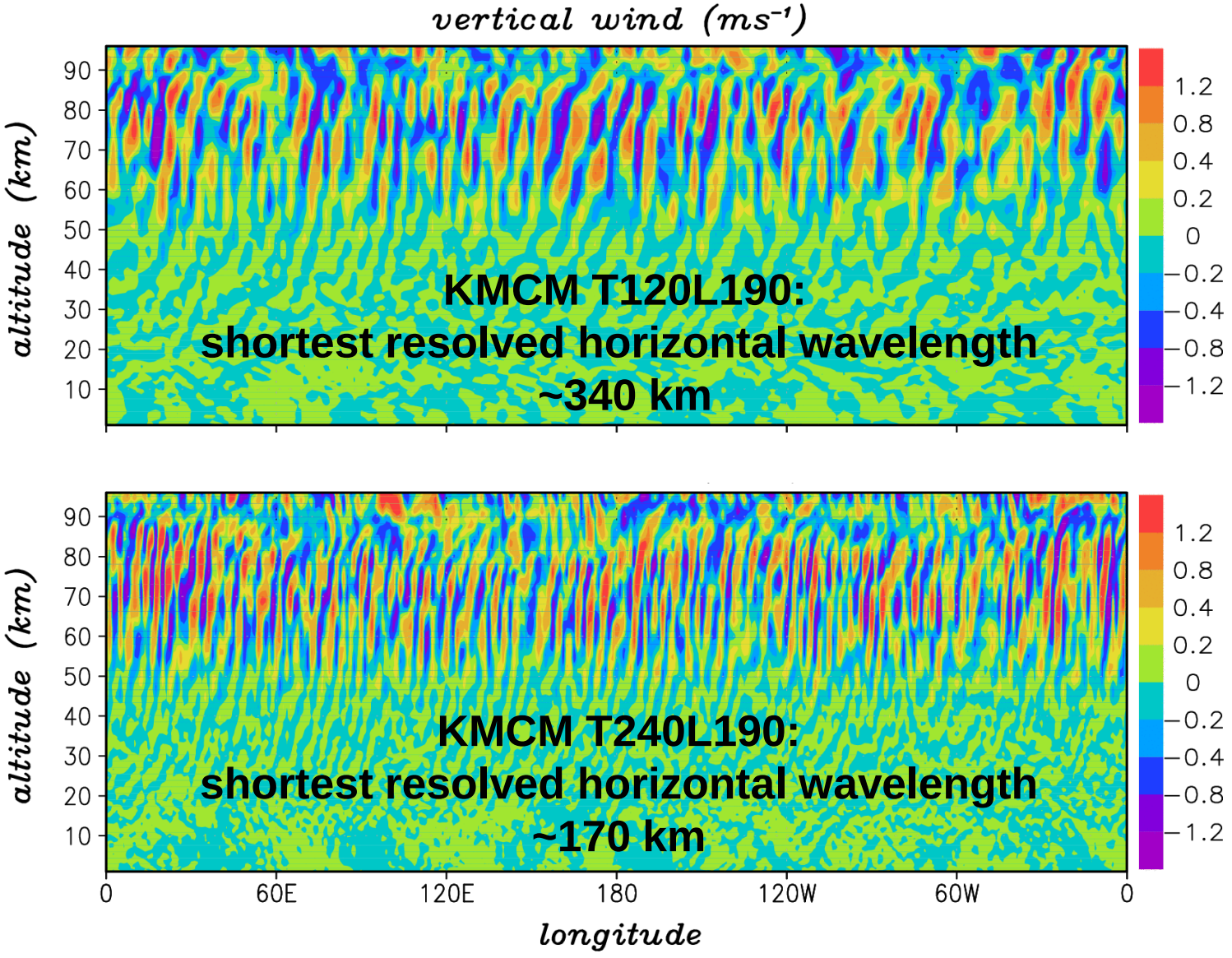

For higher resolution, the simulated gravity waves have smaller spatial scales (and higher frequencies).

Dependence of simulated GW scales on the spatial resolution

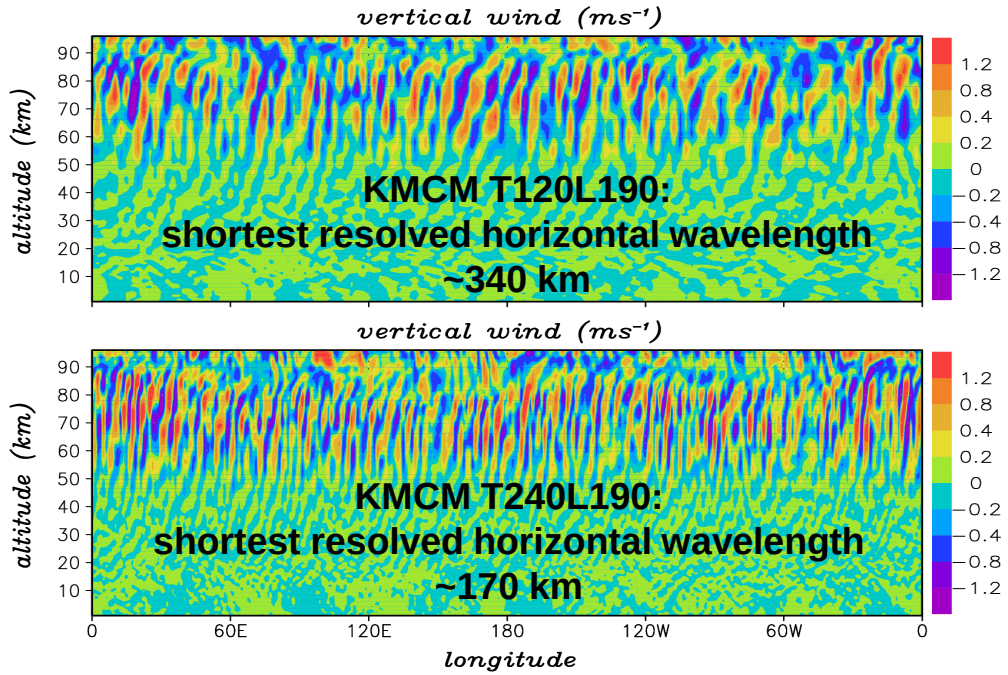

For higher resolution, the simulated gravity waves have smaller spatial scales (and higher frequencies).
As a result, smaller GW amplitudes induce similar mean-flow effects.

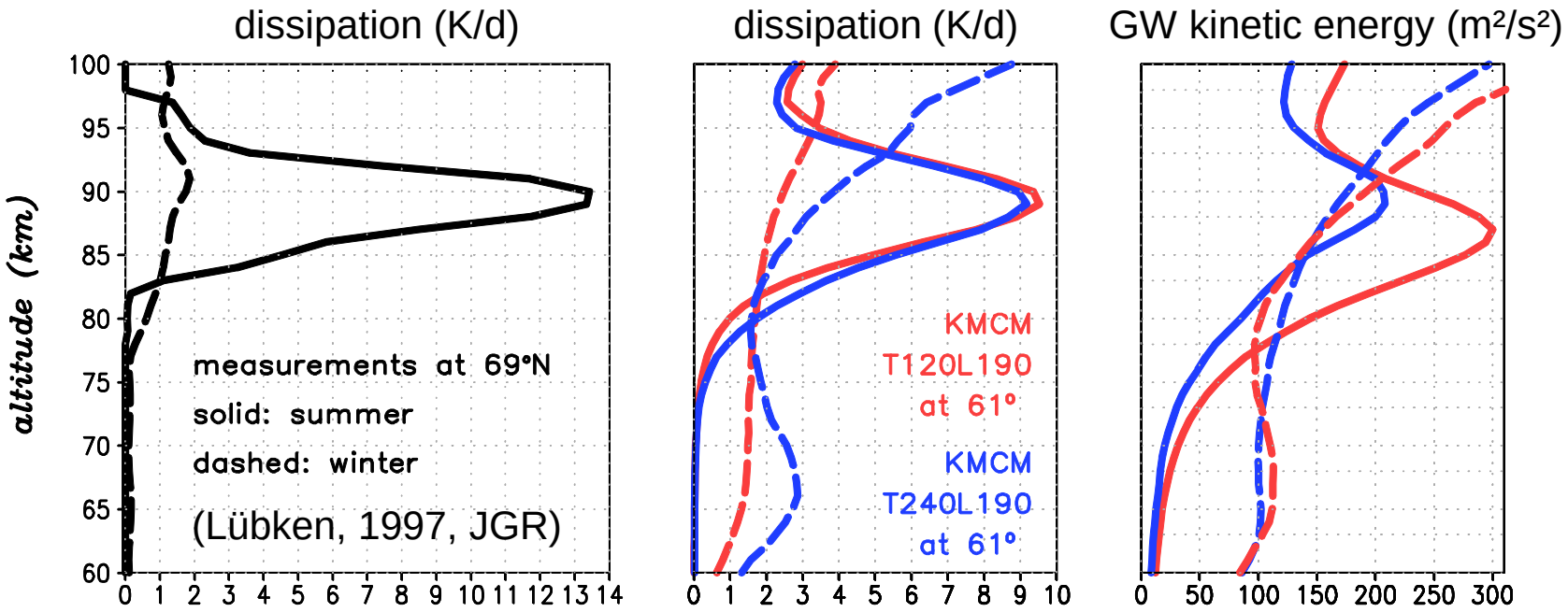

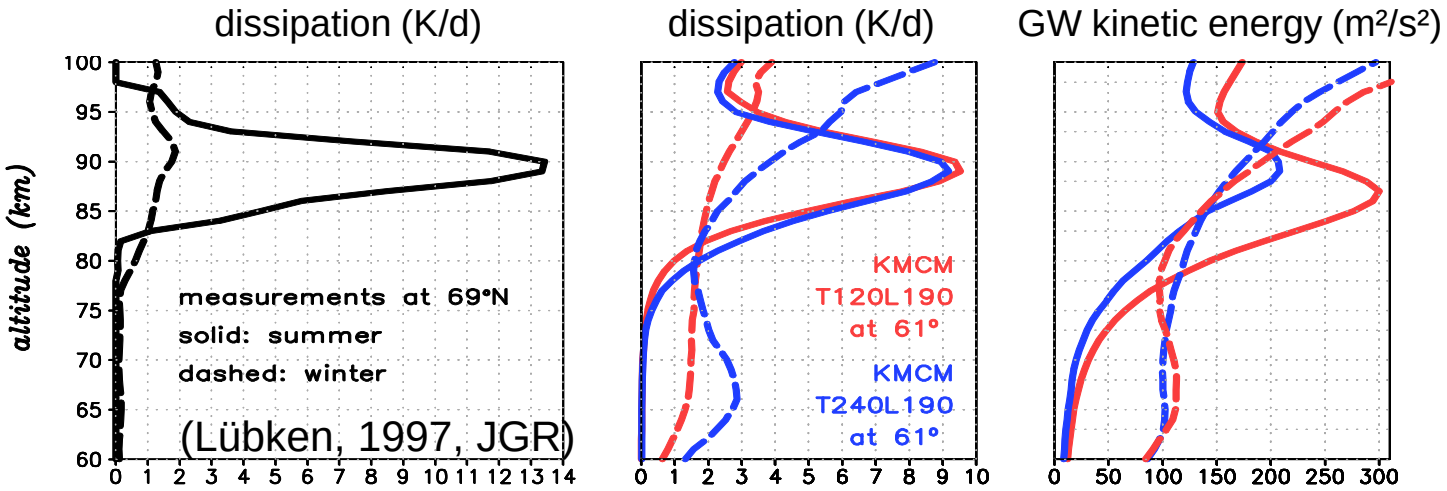

Budget for the gravity-wave kinetic energy

energy deposition

$$\partial_t \overline{\mathbf{v}^2}/2 = \underbrace{-\overline{\left((\mathbf{v}\circ\mathbf{v})\nabla\right)\cdot\mathbf{v}}}_{\text{horiz. ddv.}} \underbrace{-\frac{\overline{\partial_z\, p\, w}}{\rho_r} - \frac{\overline{g\,\rho\, w}}{\rho_r}}_{\text{adiabatic conversion}} \underbrace{-\overline{(w\,\mathbf{v})\cdot\partial_z\mathbf{v}}}_{\text{vert. adv.}} + \underbrace{\overline{\mathbf{v}\cdot\mathbf{R}}}_{\sim -\overline{\epsilon}}$$

negligible

negligible

Spectral kinetic energy in an atmospheric GCM

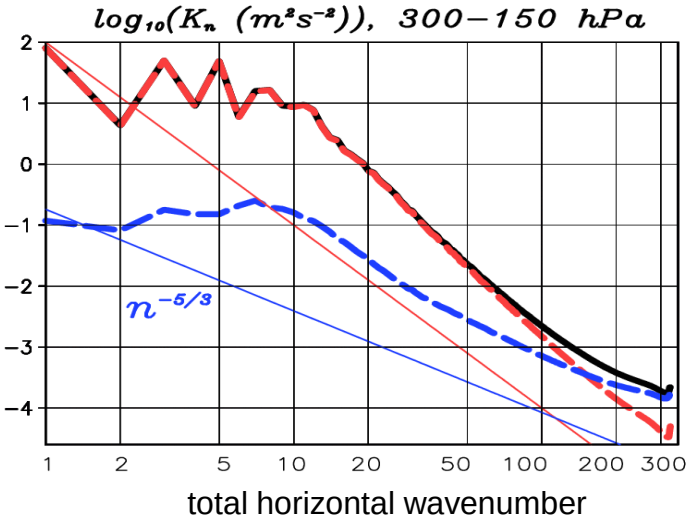

spectral representation of the horizontal wind:

$$\mathbf{v} = -\sum_{n=1}^{N} \frac{a^2}{n(n+1)} \sum_{m=-n}^{+n} \left(\xi_{nm} \, (\mathbf{e}_z \times \nabla \, Y_{nm}) + D_{nm} \, \nabla \, Y_{nm} \right)$$

$$= \qquad \mathbf{v}^{rot} \qquad + \qquad \mathbf{v}^{div}$$

height-dependent global mean and spectral kinetic energy per unit mass:

$$K = (4\pi)^{-1} \int \frac{\mathbf{v}^2}{2} \, d\Omega = \sum_{n=1}^{N} K_n$$

$$K_n = \frac{a^2}{8\pi \, n(n+1)} \sum_{m=-n}^{n} \left(\xi_{nm}^2 + D_{nm}^2 \right)$$

analogously for enstrophy: $Z_n = \frac{1}{8\pi} \sum_{m=-n}^{n} \xi_{nm}^2$

Spectral budgets

$$\dot{K}_n = \frac{a^2 \,/\, 4\pi}{n(n+1)} \sum_{m=-n}^{n} \left(\dot{\xi}_{nm}\, \xi_{nm} + \dot{D}_{nm}\, D_{lnm} \right) , \quad \dot{Z}_n = \frac{1}{8\pi} \sum_{m=-n}^{n} \dot{\xi}_{nm}\, \xi_{nm}$$

compute $\dot{\xi}_{n\,m}$ and $\dot{D}_{n\,m}$ for different contributions to the horizontal momentum equation via spectral transformation

→ **spectral tendencies and spectral fluxes**:

HA	complete horizontal advection	$\dot{K}_n^{HA}$	$\sum_{\tilde{n}=n}^{N} \dot{K}_{\tilde{n}}^{HA}$
HA2	(quasi-)2D horizontal advection (using just $\mathbf{v}^{rot}$ instead of $\mathbf{v}$)	$\dot{K}_n^{HA2}$ $\dot{Z}_n^{HA2}$	$\sum_{\tilde{n}=n}^{N} \dot{K}_{\tilde{n}}^{HA2}$ $\sum_{\tilde{n}=n}^{N} \dot{Z}_{\tilde{n}}^{HA2}$
AC	adiabatic conversion	...	...
VA	vertical advection	...	...
MD	momentum diffusion	...	...

Continuous spectral fluxes (T330L100)

(Brune & Becker, 2013, JAS)

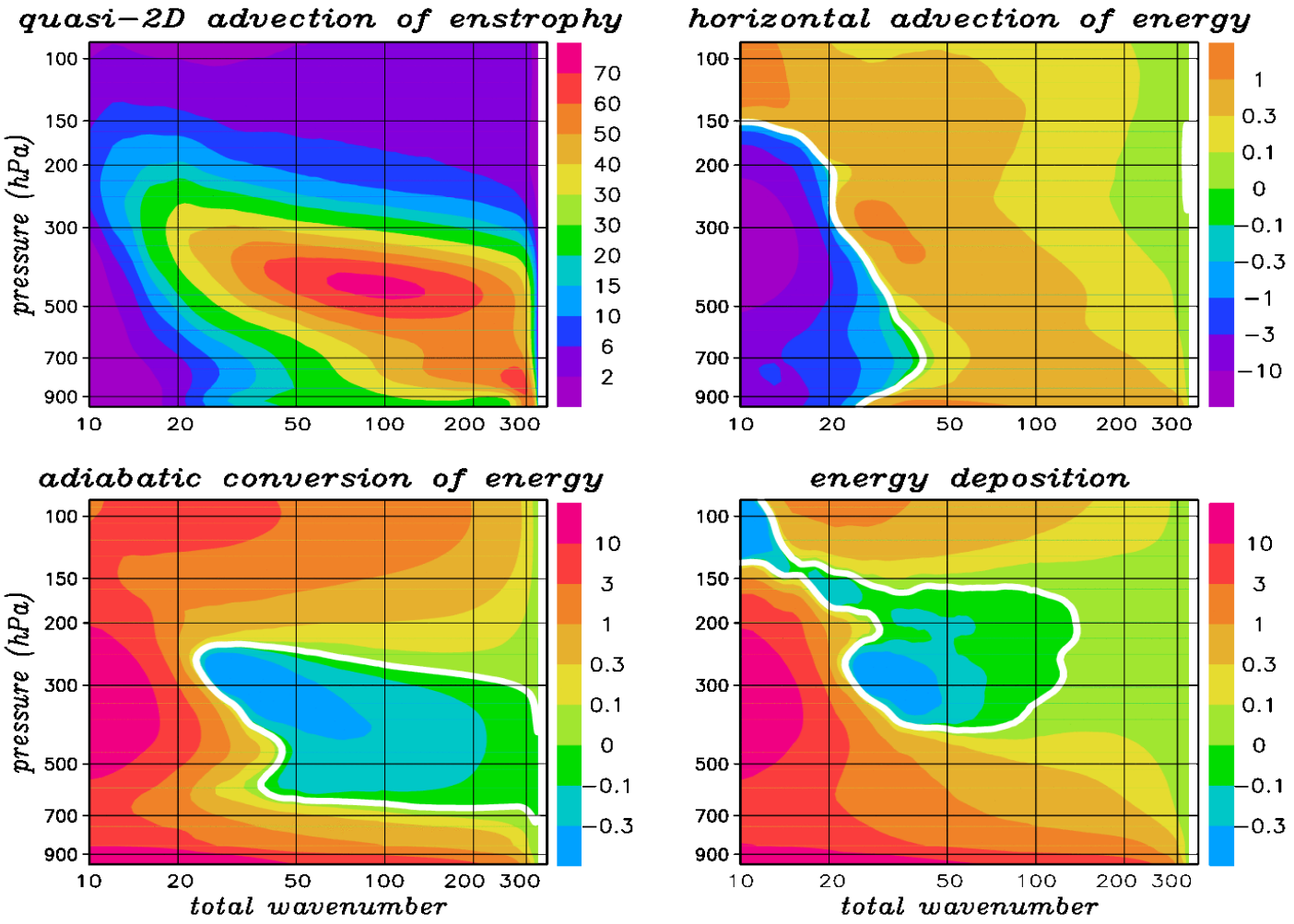

- horizontal enstrophy and energy cascades as expected
- spectral flux due to adiabatic conversion indicative of stratified turbulence
- almost no energy desposition by the mesoscales in the upper troposphere:

Consequences

- Stratified turbulence with the scaling $l_z = l_h^{1/3} \varepsilon^{1/3} / N$ is a physically motivated concept for the macro-turbulent behavior in the mesoscales above the boundary layer (possibly up to the lower thermopshere).

- Any macroturbulent diffusion for this inertial range must not only fulfill the conservation laws, but must in addition be scale-invariant.

- Such a closure has only recently been proposed (Schaefer-Rolffs, Knöpfel & Becker, Meteorol. Z, 2015; Schaefer-Rolffs & Becker, MWR, 2012 and 2015 subm.).

A new scale-invariant closure for truncation in the mesoscales

Diffusion coefficients for horizontal momentum

$$K_h = {l_h}^2 |\mathbf{S}_h| \gg K_z = {l_z}^2 |\partial_z \mathbf{v}|, \qquad l_z \propto \sqrt{l_h}$$

$$\mathbf{S}_h = \nabla \circ \mathbf{v} + (\nabla \circ \mathbf{v})^{\mathrm{T}} - \mathbf{1}(\nabla \cdot \mathbf{v})$$

$${l_h}^2 = \frac{|\widetilde{\mathbf{v} \circ \mathbf{v}} - \tilde{\mathbf{v}} \circ \tilde{\mathbf{v}} - \mathbf{1}(\widetilde{\mathbf{v}^2} - \tilde{\mathbf{v}}^2)/2|}{\left|\left(\frac{\widetilde{\Delta_h}}{\Delta_h}\right)^2 |\widetilde{\mathbf{S}_h}| \widetilde{\mathbf{S}_h} - |\widetilde{\mathbf{S}_h| \mathbf{S}_h}\right|}$$

Diffusion coefficients for any scalar variable C (sensible heat, tracer)

$$K_h \to \frac{K_h}{\gamma_h}, \qquad \frac{1}{\gamma_h} = \frac{{l_{C,h}}^2}{{l_h}^2} = \frac{1}{{l_h}^2} \frac{|\widetilde{C\mathbf{v}} - \tilde{C}\tilde{\mathbf{v}}|}{\left|\left(\frac{\widetilde{\Delta_h}}{\Delta_h}\right)^2 |\widetilde{\mathbf{S}_h}| \widetilde{\nabla C} - |\widetilde{\mathbf{S}_h| \nabla C}\right|}$$

$$K_z \to \frac{K_z}{\gamma_z}, \qquad \frac{1}{\gamma_z} \propto \frac{l_{C,h}}{l_h} = \frac{1}{\sqrt{\gamma_h}}$$

Conventional Smagorinsky Model completed by hyperdiffusion

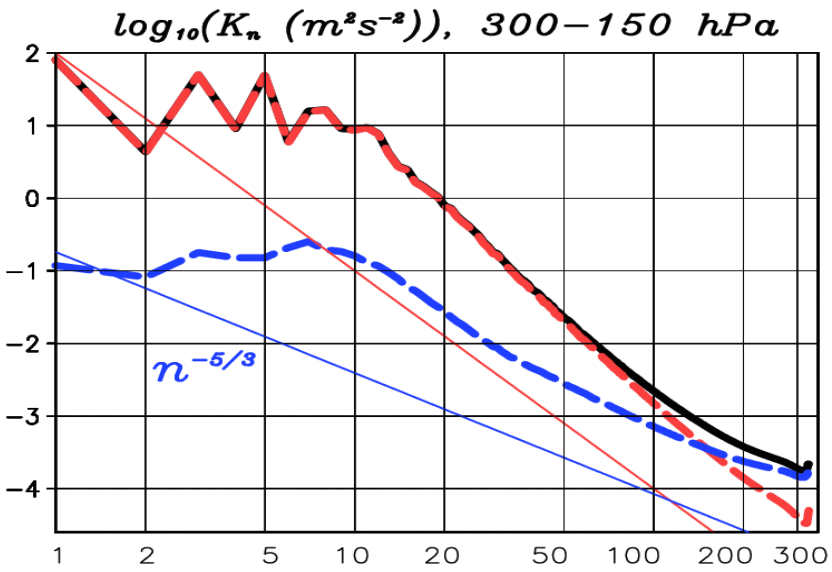

New DSM

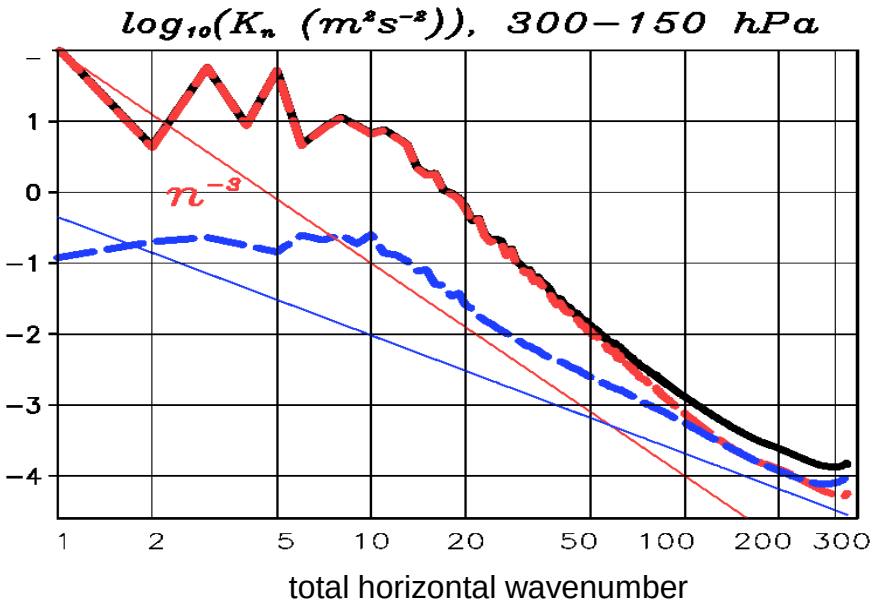

KMCM as a mechanistic climate model

- Resolutions: T32L70 , T42L110, or T120L190, all up to ~125 km
- Turbulent diffusion consistent with conservation laws and interacting with parameterized GWs
- Doppler-spread parameterization for non-orographic GWs (Hines, 1997, JASTP) and McFarlane (1987, JAS) scheme for orographic GWs: with consistent treatment of turbulent diffusion and direct thermal effects (Becker & McLandress, 2009, JAS; B. Wolf, diploma thesis, Univ. of Rostock 2013)
- Tracer transport based on the spectral transform method (Schlutow et al., 2014, JGR): Energy conserving tropospheric moisture cycle
- Continuous computation of radiative transfer from the surface up to the lower thermosphere, including deviations from LTE and the gray limit (Knöpfel & Becker, 2011, JQSRT; Becker et al., 2015, JASTP, subm.) → complete energy budget of the surface (slab ocean with prescribed oceanic heat-flux convergence; land-sea masks for surface heat capacity, albedo, and relative humidity)

Surface parameters and moisture cycle

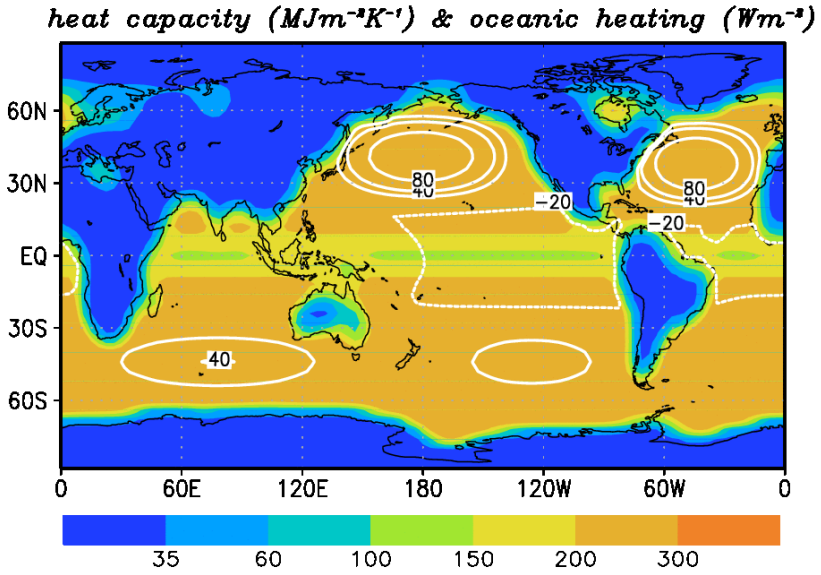

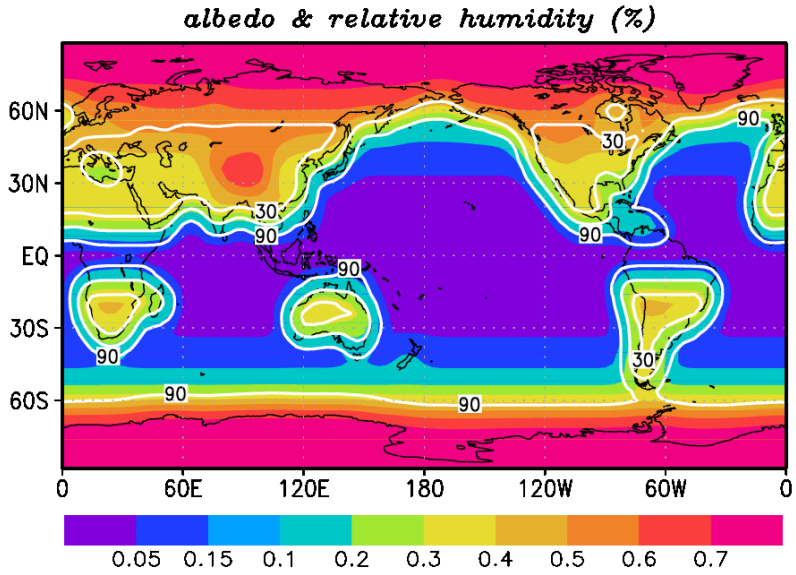

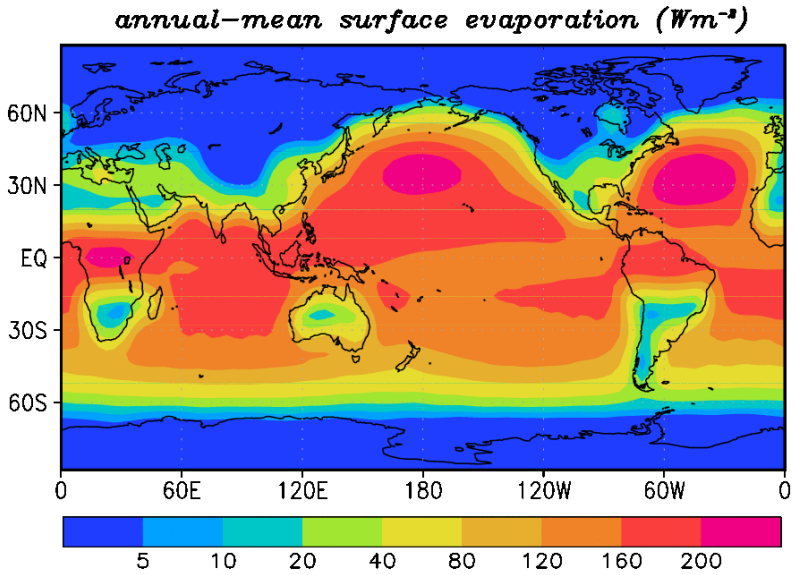

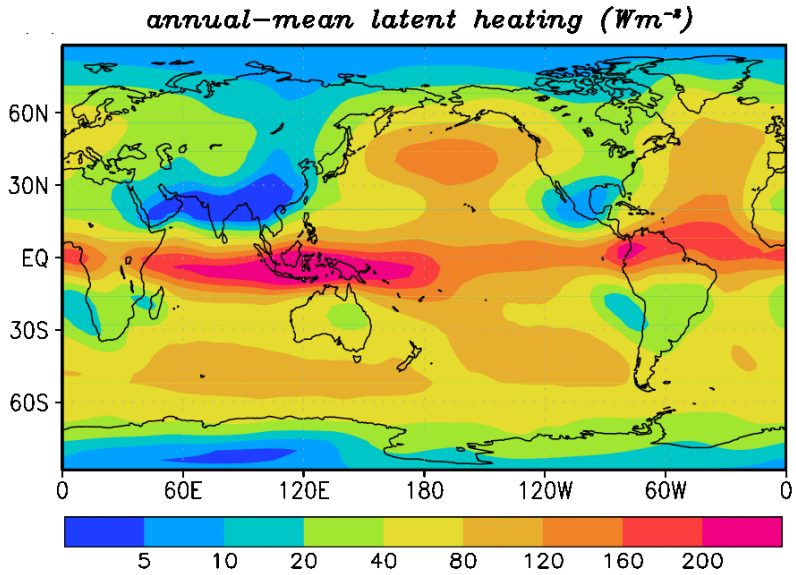

Moisture cycle in the zonal mean

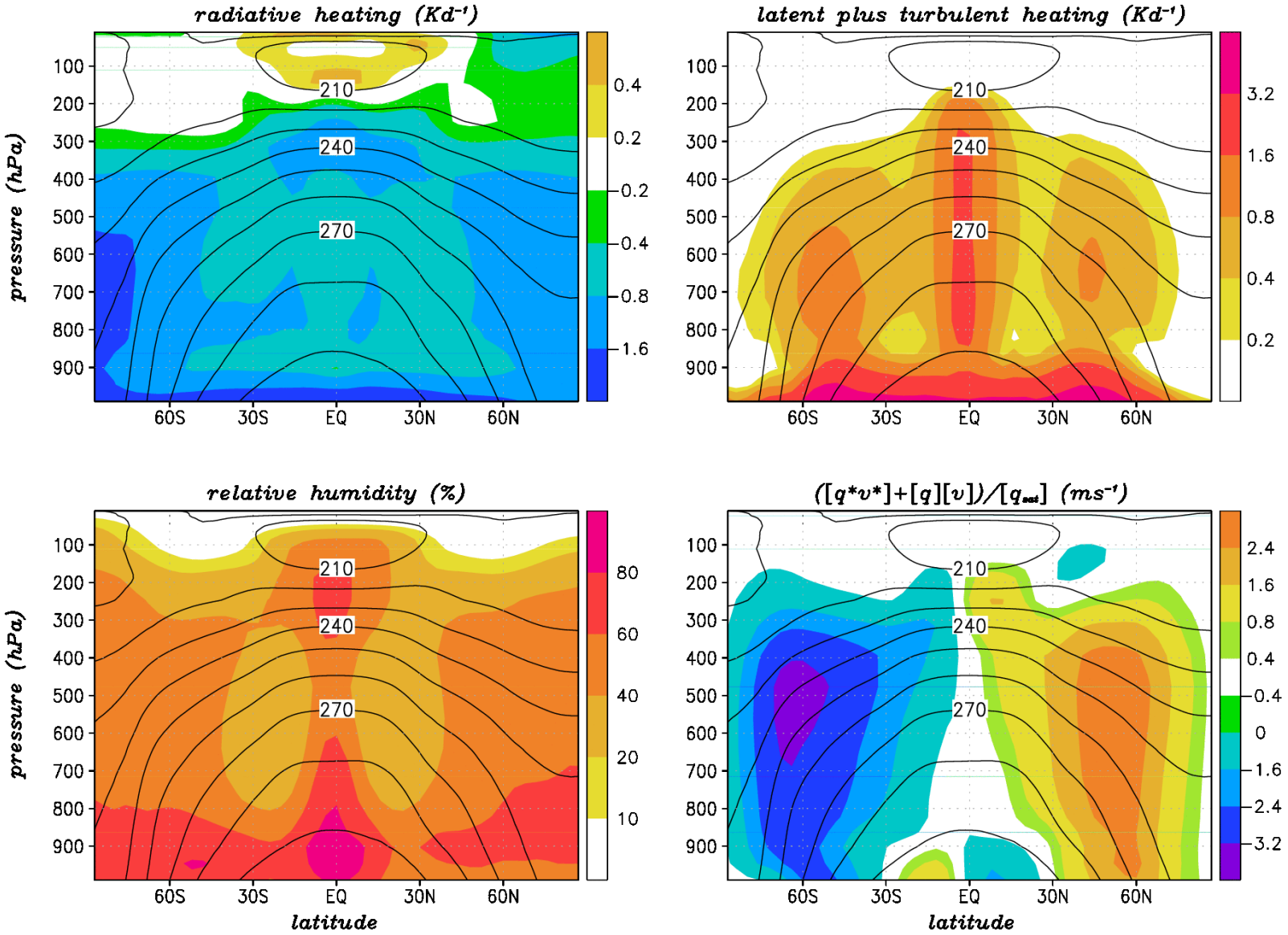

DJF stationary waves

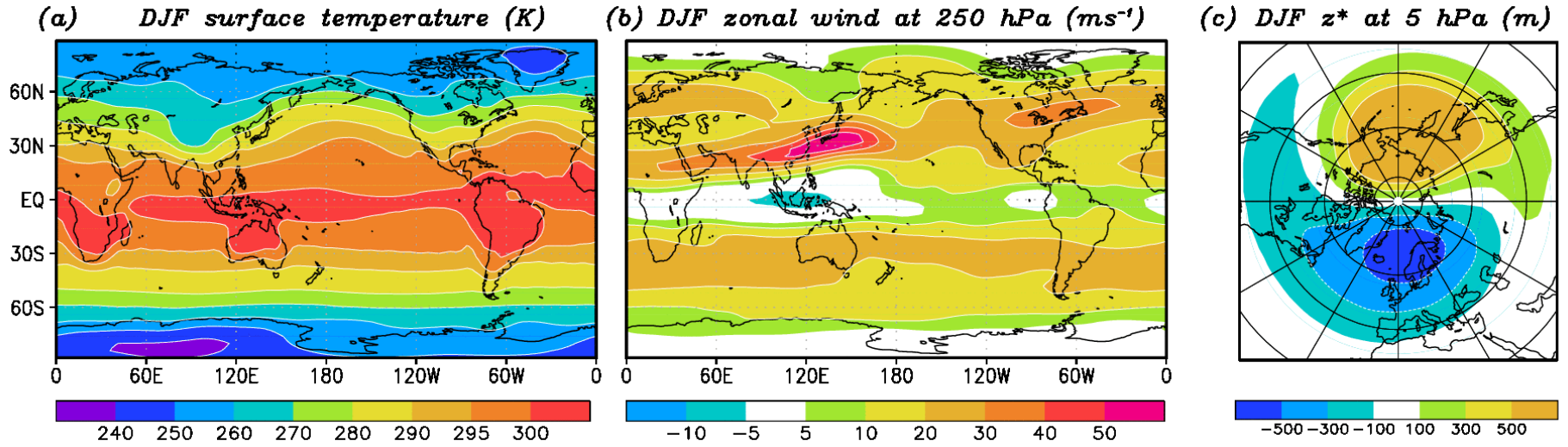

Zonal-mean climatology during July and January

July

January

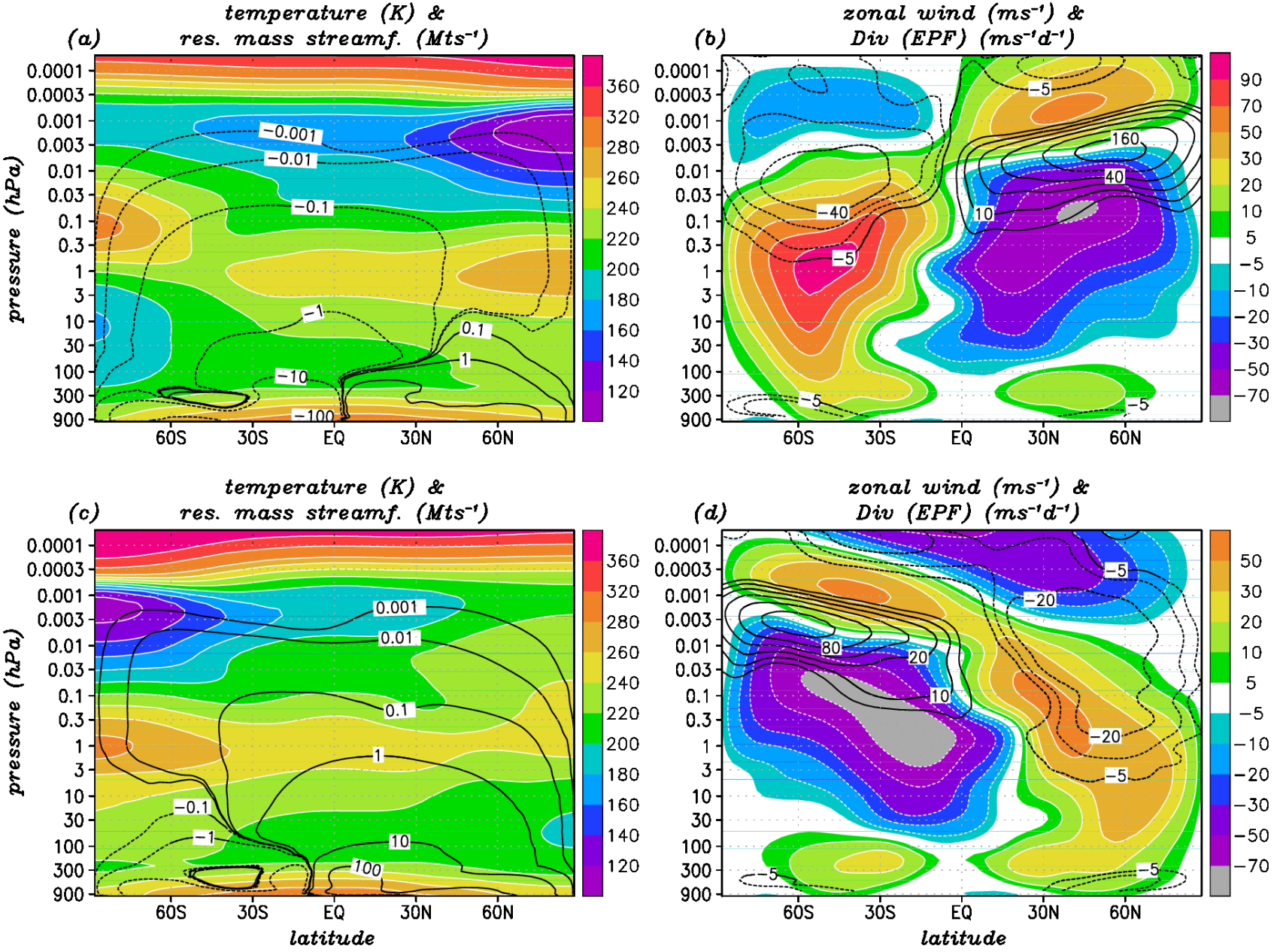

Simulated annual-mean radiation budget at the top of the atmosphere

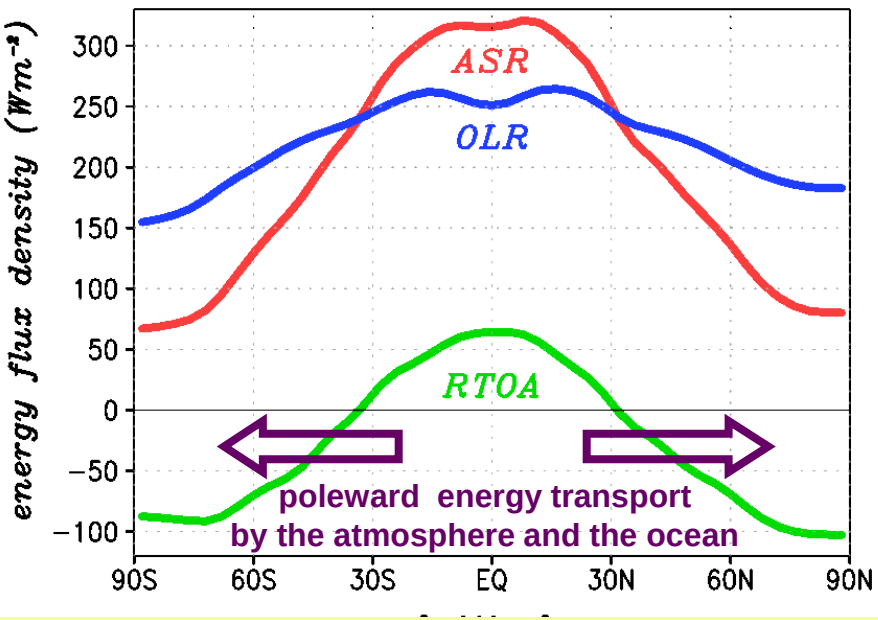

OLR = outgoing long-wave radiation

ASR = absorbed solar radiation

RTOA = ASR – OLR
= net downward radiation

The KMCM is energetically consistent because each conversion preserves energy. Errors are due to aliasing only.

- intensity of the Lorenz energy cycle ~ 1.9 Wm^{-2}
- latent + sensible surface heat flux ~ 80 Wm^{-2}
- mean ASR ~ mean OLR ~ 230 Wm^{-2}
- SR absorbed by the surface / atmosphere ~ 152 / 78 Wm^{-2}
- mean error in the RTOA ~ -0.20 Wm^{-2}
- evaporation - condensation ~ -0.15 Wm^{-2}
- error of the surface energy budget ~ -0.14 Wm^{-2}

Mean annual cycle: Global mean budgets

radiation budget
at the top of the atmosphere

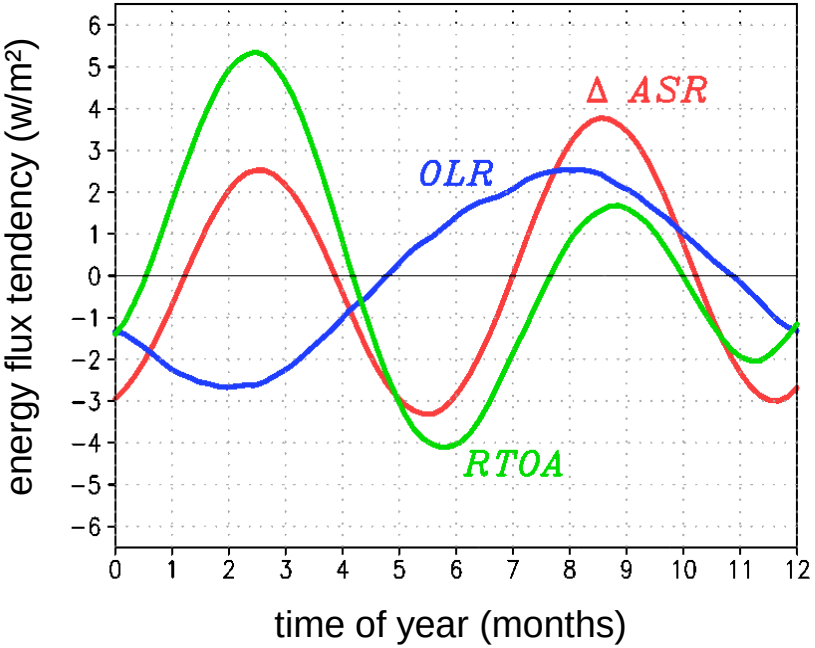

energy budget and
temperature at the surface

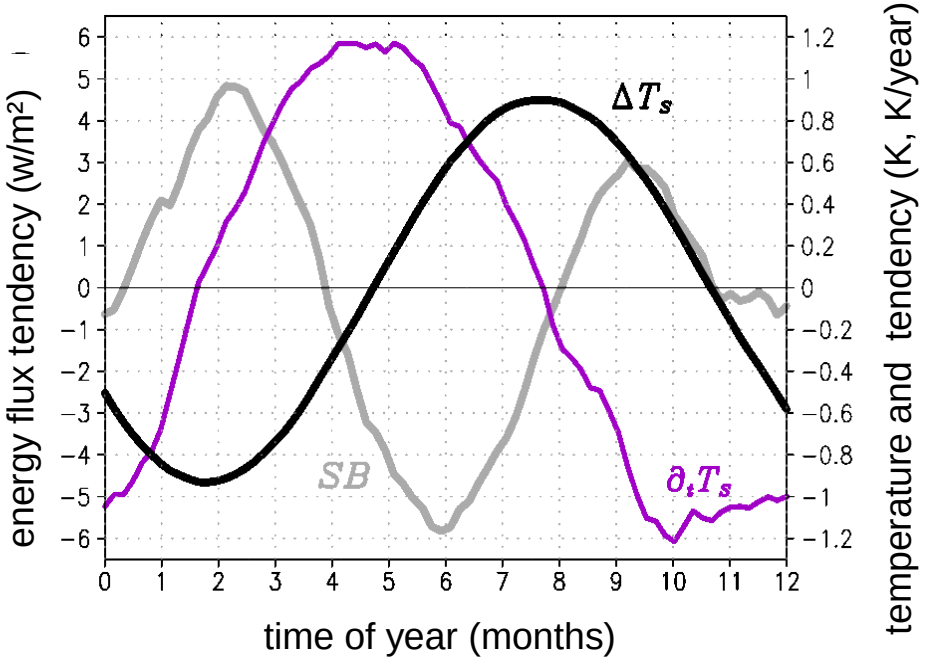

- The mean annual cycle is characterized by regular variations with heat storage/release during NH winter/summer along with global cooling/warming, giving rise to a positive/negative RTOA.
- Importance of this bottom-up causality for the RTOA in the context of the present stagnation of global warming?

Conclusions

The mesosphere/lower thermosphere (MLT, 50-110 km) is a challenging altitude range to test circulation models with regard to mesoscale dynamics and parameterizations to solve the closure problem.

Current circulation models do not converge with increased spatial resolution, presumably because of insufficient closures.

Strategy of the theory & modeling department at IAP:
Apply high resolution and aim at a physically consistent parameterization in terms of the Dynamical Smagorinsky Model and assuming an inertial regime in the mesoscales that is governed by stratified turbulence.

A mechanistic model is well suited to develop and test new closures. It can also be formulated as a semi-realistic climate model with consistent energetics by virtue of model formulation.

The annual cycle of the radiation and surface budgets may serve as a benchmark for complex climate models.

spectral fluxes of kinetic energy ($m^2/s^2/d$) owing to

horizontal advection | adiabatic conversion | energy deposition

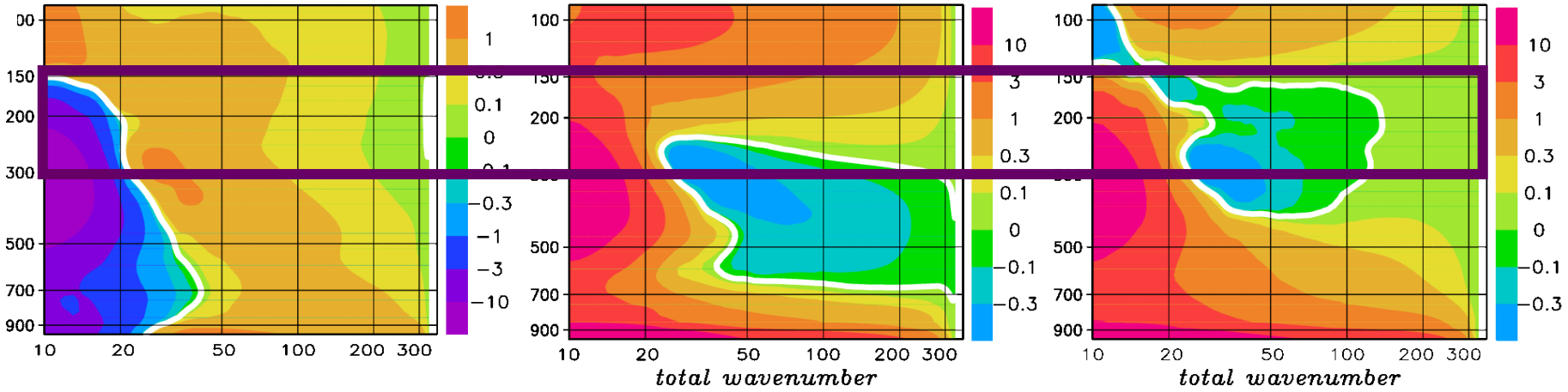

Global kinetic energy spectrum and normalized spectral tendencies
(KMCM T240/L190 with realistic gravity-wave effects in the mesosphere)

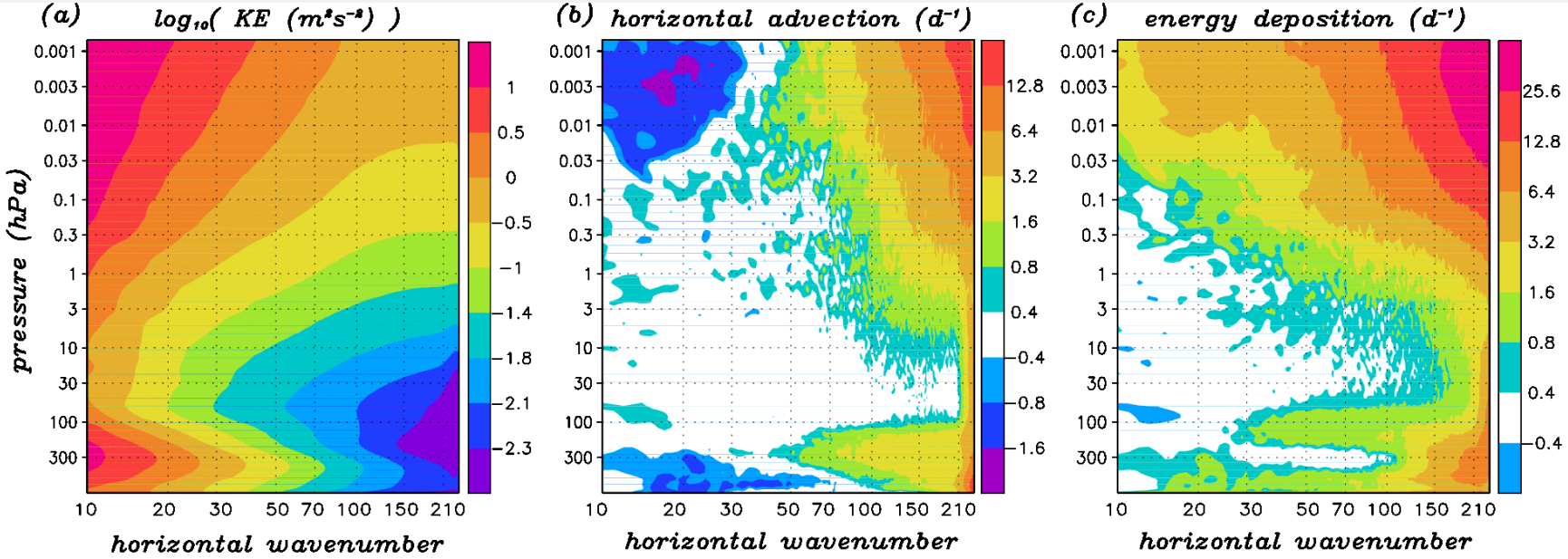

(Becker & Brune, 2014, JAS)